International Journal of Engineering & Technology, 7 (4.14) (2018) 538-543

International Journal of Engineering & Technology

Website: www.sciencepubco.com/index.php/IJET

Research paper

Effects of Boron and Carbon Added Titanium Filler on Microstructure and Mechanical Properties of Ti-15-3 Alloy Weldments

Izzul Adli Bin Mohd Arif[1], Mahesh Kumar Talari[2*], N Kishore Babu[2], Ahmad Lutfi Bin Anis[3], Muhammad Hussain Ismail[4] , Rosmamuhamadani Bin Ramli[1]

[1] Faculty of Applied Sciences, Universiti Teknologi MARA, 4045, Shah Alam, Selangor, Malaysia
[2]Department of Metallurgical and Materials Engineering National Institute of Technology Warangal, Telangana 506004 India
[3]Faculty of Applied Sciences, Universiti Teknologi MARA 94300 Kota Samarahan, Sarawak, Malaysia
[4]Faculty of Mechanical Engineering, Universiti Teknologi MARA, 40450, Shah Alam , Selangor, Malaysia
** Corresponding author E-mail: talari@nitw.ac.in*

Abstract

Microstructural and mechanical properties beta Titanium (β-Ti) weldments can be improved by grain refinement and formation of insoluble precipitates in the weld. This paper reports the effect of Boron (B) and Carbon (C) addition to Ti-15V-3Cr-3Sn-3Al (Ti-15-3) fillers on the microstructural and mechanical properties of Ti-15-3 gas tungsten arc weldments. X-ray diffraction and scanning electron microscopic analysis revealed the presence of β-Ti phase in the weldments prepared without the filler modification, while additional TiB and TiC phases are observed in the weldments prepared with fillers modified with B and C, respectively. B and C addition to the fillers has resulted in the grain refinement of the weldments and the grain size reduction is seen to be higher with the increasing B and C addition. The formation of TiB, TiC and growth restriction effect due to the presence of B and C in the filler resulted in the decreased grain size of the β-Ti weldments. Mechanical properties such as hardness and tensile strength improved as the amount of B and C addition increased. The improvement of mechanical properties is contributed by the grain refinement and the formation of TiB and TiC precipitates in weldments.

Keywords: *Boron, Carbon, Grain Refinement; GTAW; Ti-15-3*

1. Introduction

The alloying elements that are added to titanium can be classified as α stabilisers and β stabilisers [1]–[3]. Though β phase in pure titanium is a high temperature phase, room temperature beta titanium (β-Ti) alloys can be formed by the addition of β stabilising elements, which lower the β transus temperature. β-Ti alloys does not undergo allotropic transformation upon quenching to room temperature resulting in retained metastable β phase which can be further hardened to improve hardness and tensile strength by suitable thermomechanical and ageing treatments [3]. Besides that, β-Ti is reported to display corrosion resistance on par or better compared to other classes of Ti alloys [1], [2]. The high strength to weight ratio of β-Ti alloys such as Ti-10-2-3 alloy makes these alloys suitable for applications such as landing gear of aircraft Boeing 777 in aerospace applications [4]. The other example of β-Ti alloys that are used in aerospace structural applications are Ti-13-11-3 alloys, which was used in SR-71 "Black Bird" aeroplane component due to high thermal stability of the alloys [3].

Ti-15-3 castings were used in the cargo handling area and for auxiliary power units (APU) vibration isolator mount in Boeing 777 [3]. Ti-15-3 possesses high specific strength, excellent hardenability and corrosion resistance. These alloys are heat-treatable, suitable to undergo cold work process in solution-treated condition and display excellent fatigue properties [1], [3].

Most of β-Ti applications involve the welding methods such as gas tungsten arc welding (GTAW) and electron beam welding (EBW). GTAW is more preferred because it is more economical. Among the various methods suggested to increase the weldability of the β-Ti are pulsed current welding (PCW) GTAW and usage of proper fillers [5], [6]. The fusion zone (FZ) and heat affected zone (HAZ) in welded β-Ti show low-strength retained β structure. Increased β stabiliser elements in advanced Ti alloys tend to reduce weldability [5]. Welding of titanium alloys is usually associated with the coarse columnar grain structure in the FZ and HAZ which is caused by the prevailing thermal conditions during solidification of the weld metal [7], [8]. It was found that heat treated β alloy weld microstructures in Ti-5AI- 5Sn-2Zr-4Mo6 and Ti-6AI-4V showed a larger prior beta grain size [9], [10]. This causes the mechanical properties of the weldment to become poor. Alternative methods to improve weldability include inoculation, electromagnetic stirring (EMS) and modification of welding parameters.

Addition of elements such as boron (B), carbon (C) and beryllium (Be) has been employed to modify the microstructure of conventional as-cast Ti alloys. Addition of B into pure Ti alloys has been reported to cause dramatic grain refinement [11]. The grain refinement is due to reduction of prior-β grain size or α-grain size. Boron addition into Ti-6-4 causes a change in solidification behaviour. It was proven that the cast grain structure changes from columnar to equiaxed structure at minimum solidification rate of 20 mm/h with less than 0.1 wt.%. B addition

[12]. Finer grain size can improve the mechanical properties of the material by impeding dislocation motion and increase the strength of material. Significant improvements in the mechanical properties due to refined cast microstructure have been reported mostly for the α-β alloy with the addition of B [13]–[17]. Grain refinement and increase in mechanical properties have been reported in β Ti with the addition of B [15], [18]. Similarly, the addition of B in Ti-21S and Ti-15-3 alloys has led to the refinement of the cast structure and resultant improvement in strength and elongation-to-failure [15].

The microstructure of β-Ti alloy can also be enhanced by C additions where refinement in the microstructure is expected to improve the mechanical properties. Sarkar et al (2011) reported that the distribution of TiC in the matrix is finer and more uniform compared to distribution of TiB [4]. Improvement of mechanical properties of C added Ti alloys is due to the grain refinement and the formation of hard TiC precipitates in the matrix [4], [17], [19]. Du et al (2014) found that the addition of C into the β-Ti alloy provide almost similar effect as addition of B [17]. It was also found that the addition of C and B causes the formation of TiC and TiB precipitates, respectively in the microstructure of β-Ti. Bermingham et al (2008) have confirmed that the formation of TiB can assist in nucleation of α-phase during the ageing treatment [11]. Modification of weld filler by the addition of B and C may help refine the grain and increase the strength of the weld joint without affecting the mechanical properties of the base metal (BM). This paper reports the effect of B and C added Ti-15-3 filler on microstructure and mechanical properties of Ti-15-3 alloy GTAW weldments.

2. Experimental Procedure

Ti-15-3 rod, graphite chips and B chips were weighted prior to melting of Ti-15-3-1wt. % C and Ti-15-3-1wt. % B master alloys by argon arc melting method. The master alloy was then used to prepare samples with the composition of Ti-15-3-0.5B, Ti-15-0.25B, Ti-15-3-0.5C and Ti-15-0.25C by adding Ti-15-3 rod to the master alloy. Samples were melted using a laboratory argon arc melting furnace with a non-consumable tungsten electrode on a water-cooled Cu hearth. Samples were melted at least 5 times by turning upside down after each melting to ensure homogeneity of the fillers. Then the rod-like fillers were sliced to obtain ±1mm thick and ±2mm height filler. The rods were sectioned using Buehler Isomet® 5000 linear precision high speed cutter.

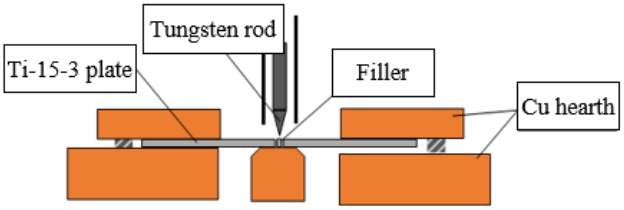

Fig. 1: Schematic diagram of the weld setup showing the Ti-15-3 base plate and the filler

Welding was performed using pulsed current GTAW for Ti-15-3 plate with 1) B added Ti-15-3 filler, 2) C added Ti-15-3 filler and 3) without filler (autogenously). Schematic diagram of the experimental setup prior to weld is shown in Figure 1. Speed of the torch was set to 60mm/min while the welding current and frequency were 129A and 120Hz, respectively. Base current was set to 60% from the peak current with the pulse-on- time of 30%. Welded Ti-15-3 plates then were cut using Wire Cut Electrical Discharge Machine (EDM) to obtain the required shape and size for microstructural and mechanical properties analysis. EDM method was used to minimize the further strain involvement and material loss. The samples were metallographically prepared prior to etching using Kroll's reagent (5 ml HF + 10 ml HNO3 + distilled water) at room temperature for microstructural observation. Optical microscopic analysis was carried out using Olympus BX60 microscope. Microstructures of etched samples were obtained using a Zeiss Supra 40VP field emission scanning electron microscope (FESEM). The phase identification analysis was performed using a PANalytical X-ray diffractometer (XRD) with Cu Ka radiation. XRD measurements were conducted with step scan (2Θ) from 20° to 90° with an increment of 0.02°. Image J software was employed for the grain size measurement of all the alloys from optical micrographs. Transverse and longitudinal (all-weld) tensile sample were cut using EDM technique for the tensile testing. The samples were cut according to ASTM E8-09 specification. The test was carried out at the room temperature using Universal tester. Vickers hardness measurements were carried out using Shimadzu HMV-2 microhardness tester with a load of 0.5 kg and dwell time of 15s.

3. Results and Discussions

The XRD data obtained from FZ of weldments prepared using B and C added fillers are shown in Figure 2(a) and Figure 2(b), respectively. XRD pattern of Ti-15-3 autogenous weldments show only β phase in the microstructure. On the other hand, the as-welded of Ti-15-3 with B and C added fillers showed the formation of TiB and TiC phases in the FZ, respectively.

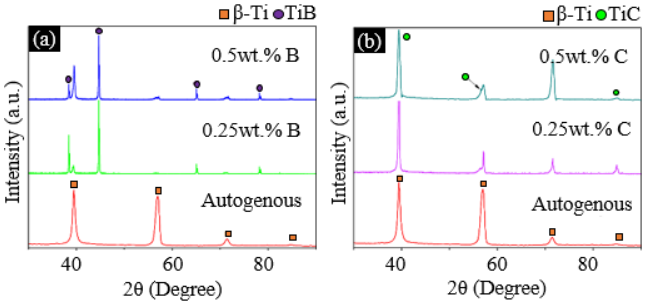

Fig. 2: XRD patterns of Ti-15-3 weldments prepared using (a) B added and (b) C added Ti-15-3 fillers

Macrograph of the welded plates in Figure 3 shows that the grain size of the BM is finer compared to the FZ. Compared to the BM, HAZ showed coarser grains indicating grain growth due to heat dissipation from adjacent fusion zone during welding. Solidification at FZ was initiated by epitaxial growth from the interface of unmelted HAZ and FZ [20]

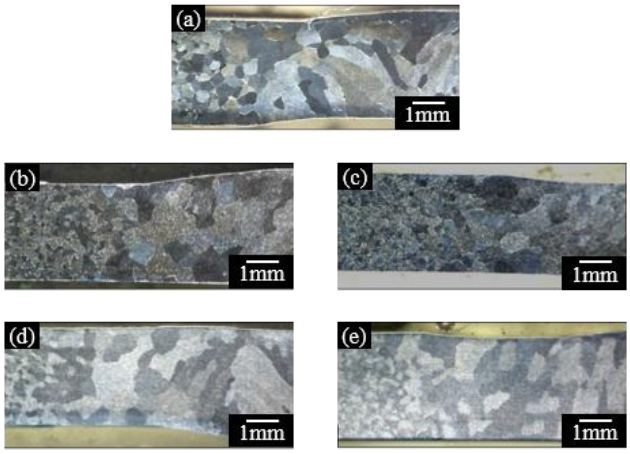

Fig. 3: Optical macrographs of transverse cross sections of Ti-15-3 welds prepared using (a) autogenous, (b) Ti-15-3-0.25wt.% B, (c) Ti-15-3-0.5wt.% B, (d) Ti-15-3-0.25wt.% C and (e) Ti-15-3-0.5wt.% C fillers

Optical micrographs for all weldments are shown in Figure 4. The grain size is seen to decrease as the wt. % of B and C in the filler

increases. Table 1 shows the average grain size values measured from the optical micrographs using image J software for each sample.

Table 1: Average Grain size of Ti-15-3 weldments

Fillers	Average grain size of FZ
No filler (autogenous)	~212.148
Ti-15-3-0.25wt.% B	~171.254
Ti-15-3-0.5wt.% B	~150.768
Ti-15-3-0.25wt.% C	~195.764
Ti-15-3-0.5wt.% C	~172.778

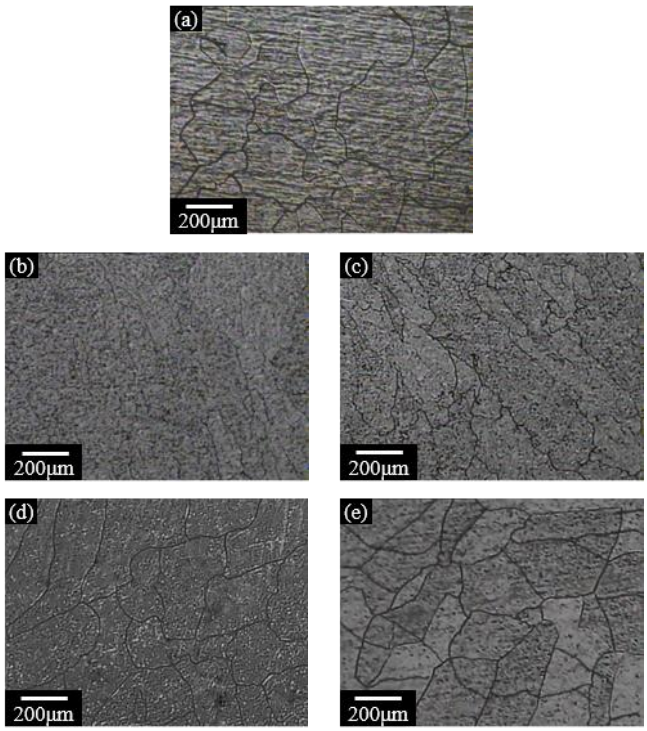

Fig. 4: Optical micrographs of Ti-15-3 welds prepared using (a) autogenous, (b) Ti-15-3-0.25wt.% B, (c) Ti-15-3-0.5wt.% B, (d) Ti-15-3-0.25wt.% C and (e) Ti-15-3-0.5wt.% C fillers

Welding process involves of melting the BM along with the fillers and resolidification upon cooling. Definition of the dilution in the welding is the change in composition of filler metal due to mixing between filler and base metal during melting process. Dilution level will determine the final composition and corresponding microstructure and properties of the fusion zone [21]. The dilution is given by

$$\text{Dilution} = \frac{A_{fm}}{A_{fm}+A_{bm}} \quad (1)$$

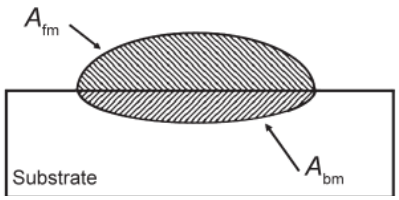

Fig. 5: Schematic illustration of dilution showing the amount of base metal melted (A_{bm}) and filler metal added (A_{fm}) in a typical fusion weld (Source:[21])

In this report, the dilution was established as 0.8 from weld FZ dimensions and the composition (wt.%) of B and C added FZ was estimated. The final wt. % of B and C in the FZ were shown in the Table 2.

Based on Ti-rich region in the Ti-B binary phase diagram [22] and Ti-C binary phase diagram [23], the eutectic composition is at ~1.64 wt.% B and ~0.315 wt. % C, respectively. Therefore, the solidification sequence for all weldments in this study is almost the same. Below wt.% of eutectic composition, the samples were hypoeutectic. For hypoeutectic composition, solidification starts with the formation of proeutectic β grains prior to the formation of TiB and TiC precipitates during eutectic reaction.

Table 2: B and C content in the FZ of the Ti-15-3 weldments

Fillers	Final composition in the FZ
No filler (autogenous)	Ti-15-3
0.25wt.% B	0.05wt.% B
0.5wt.% B	0.1wt.% B
0.25wt.% C	0.05wt.% C
0.5wt.% C	0.1wt.% C

The proeutectic β grains nucleate and grow upon cooling below liquidus temperature and while the rest of the liquid phase solidifies by eutectic reaction at eutectic temperature. Since Ti-15-3 is a metastable β Ti alloy, β phase was retained during cooling process due to higher cooling rates experienced after solidification. Inoculation of TiB and TiC seem to be impossible as the TiB and TiC phase form after the formation of proeutectic β. Hence, TiC and TiB cannot act as nucleation site β phase solidification. During proeutectic β phase solidification, concentration of B or C at solid-liquid interface increases because of B or C rejection from the solid into the melt. The resultant B-rich layer or C-rich layer retards the growth of proeutectic β and promote nucleation within the melt, resulting in smaller grain size. Therefore, the degree of latent heat production and heat extraction at the solid-liquid interface becomes significant to grain refinement. Since the rate of latent heat production is limited by the solute partitioning at the solid-liquid interface and diffusion in the melt, the influence of a solute on the grain size can be described by the growth restriction factor, Q given as [22].

$$Q = m_l (k\text{-}1)\, C_o \quad (2)$$

Where m_l is the slope of the liquidus, k is the solute partition coefficient ($k = C_s/C_l$; C_s and C_l are the solute contents of the solid and liquid phases in equilibrium, respectively), C_o is the total solute content in the alloy. Table 3 shows the values for m_l and k for various solute elements in Ti. From Ti-B binary phase diagram [22] and Ti-C binary phase diagram [23] the measured value of $m_l(k\text{-}1)$ for B and C in Ti are 66 and 38.63, respectively. At low concentrations, Al and V are highly soluble in titanium. Hence these individual solutes do not partition ahead of the solidification front unlike B and C, which segregates and results in a higher growth restriction factor (GRF). Higher GRF results in smaller grain sizes values in the solidified alloy.

Table 3: m_l (k−1) values for various solute elements in titanium

Element	m_l	k	$m_l(k\text{-}1)$	Reference
Al	-2.1	~1	0	[24]
Cr	-8.1	0.81	1.5	[24]
Sn	-0.8	~1	0	[24]
V	-4.7	~1	0	[24]
B	-66	0	66	[24]
C	-74.29	0.48	38.63	[23]

FESEM image from Figure 6(a) shows only β-Ti grains in the autogenous weldments. While addition of B or C into the FZ causes the formation of TiB and TiC along with the β-Ti. The introduction of C into the FZ resulted in the formation of TiC along grain boundaries. However, Figure 6(b)(c) and Figure 6(d)(e) shows the existence of TiB and TiC within the β phase. However, Bermingham et al. (2008) suggested that the partitioning of B also could result in TiB intermetallics to be found in the interdendritic regions[11]. Thus, it can be suggested that the TiB and TiC observed with in the grains of weld FZ are TiB or TiC formed in the interdendritic regions.

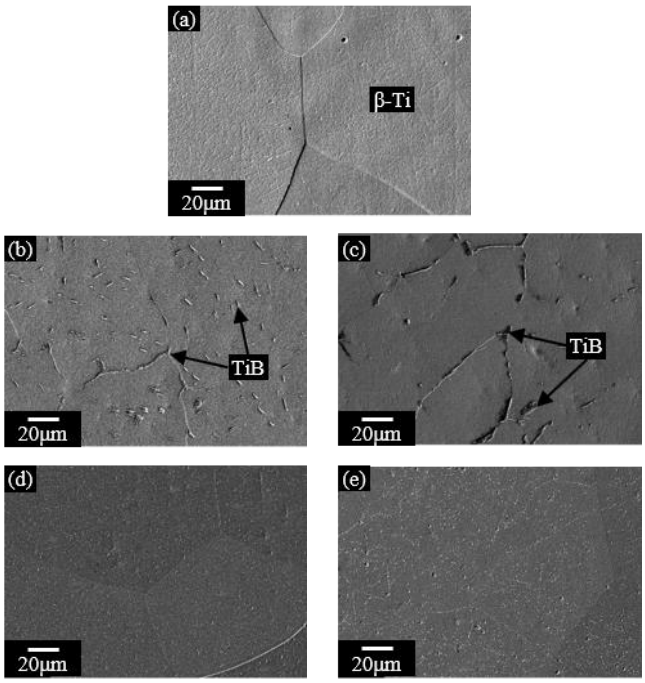

Fig. 6: FESEM micrographs of Ti-15-3 welds prepared using (a) no filler, (b) Ti-15-3-0.25wt.% B, (c) Ti-15-3-0.5wt.% B, (d) Ti-15-3-0.25wt.% C and (e) Ti-15-3-0.5wt.% C fillers

Higher magnification micrographs in Figure 7 also show TiB whiskers at the grain boundaries and within the grain. On the other hand, TiC exhibited finer precipitate morphology and more uniform distribution compared to the TiB. Carbide particle is ellipsoidal while TiB are whiskers type [4]. TiC precipitate seem more likely to form at interdendrites rather than at grain boundaries.

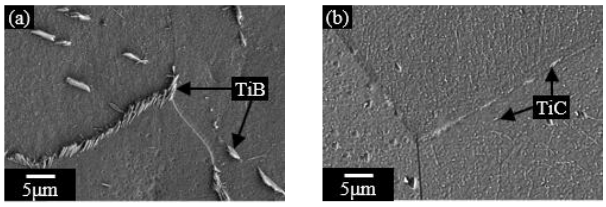

Fig. 7: High magnification FESEM micrographs of Ti-15-3 welds prepared using (a) Ti-15-3-0.25wt.% B, (b) Ti-15-3-0.25wt.% C fillers

Figure 9 shows the microhardness profile from BM to FZ for all welds. The hardness value increases from BM towards FZ. Vickers hardness of FZ in welds using filler Ti-15-3-0.5B showed highest value (352 ± 8 HV) followed by the FZs prepared using Ti-15-3-0.5C (345 ± 9 HV), Ti-15-3-0.25B (326 ± 10 HV) and Ti-15-3-0.25C (320 ± 8 HV) fillers. FZ of autogenous weld shows the lowest Hardness value (278 ± 8 HV).

The increases in the hardness of the welds caused by several factors. The increase in hardness for welds prepared with modified fillers is due to the grain refinement and the formation of TiB or TiC precipitates at grain boundary of β Ti-phase and within the grain. Based on Hall-Petch equation, the amount of stress required to transmit the dislocation through the boundary increase as the grain size become finer [25] .

$$\sigma_y = \sigma_i + kd^{-1/2} \quad (3)$$

where σ_i is the yield strength at 'infinite' grain size (single crystal), k is the Hall-Petch constant, and d is the mean grain diameter. Finer grain size restricts dislocation movement and slip in the grains resulting in increased hardness. Formation of precipitates in the matrix provide obstacle to the dislocation movement during plastic deformation as dislocations have either to bend around or bypass the precipitate for further deformation which necessitates higher forces [25]. Formation of TiB or TiC precipitates may improve the hardness of the sample by Orowan strengthening mechanism. During dislocation motion, if particle is hard then dislocations will bypass the particle either by Orowan looping or cross- slip and the particle will remain unchanged as shown on Figure 8. Consideration of the relationship between the applied stress and the dislocation bowing leads to the Orowan equation [26].

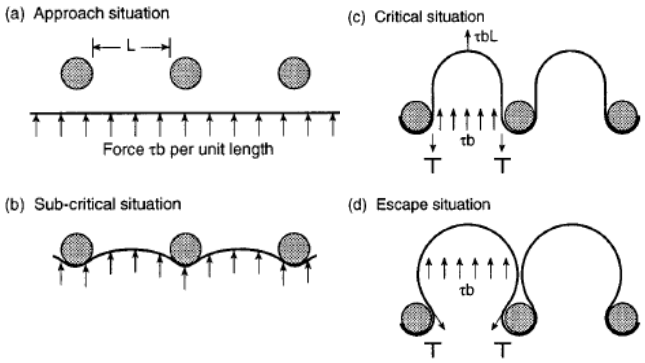

Fig. 8: Dislocation interaction with hard undeformable second phase particles: dislocation release at higher stresses may occur by Orowan looping or by cross-slip. (Source: [26])

$$Dty = Gb/L \quad (4)$$

where Dty is the increase in yield stress due to the particles, G the shear modulus of the matrix, b the Burgers vector of the dislocation and L the particle spacing. The value of L in the Orowan equation is usually considered to be the distance between particles arranged on a square grid in the slip plane [26].

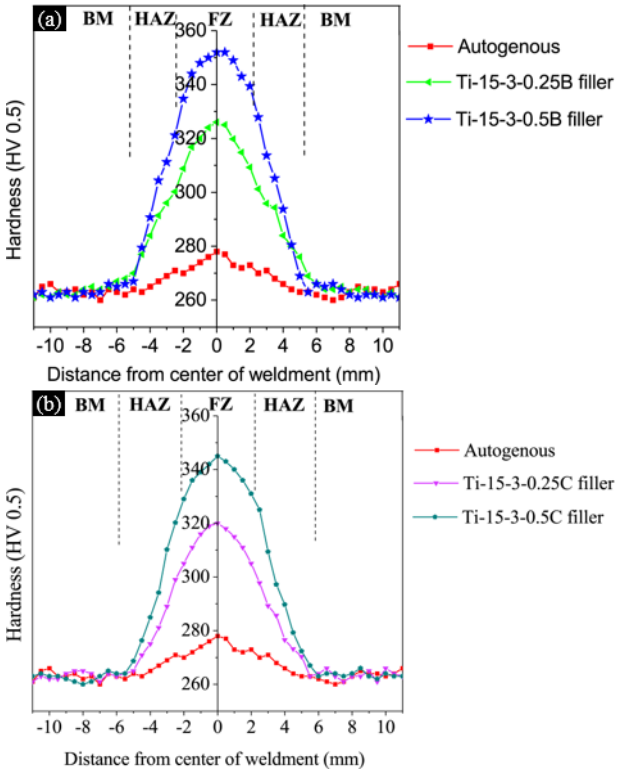

Fig. 9: Microhardness profile of the Ti-15-3 welds prepared using (a) B added fillers (b) C added fillers

Results of tensile tests on transverse tensile weld samples are plotted in Figure 10. All the tensile samples of weldments fractured within the fusion zone. Figure 10(a) shows that the welds prepared using Ti-15-3-0.5B filler exhibit higher strength

(YS = 745 ± 3 MPa, UTS = 771 ± 4 MPa) and ductility (23.1 ± 0.5 % strain) compared to welds prepared using Ti-15-3-0.25B fillers (YS = 741 ± 3 MPa, UTS = 763 ± 6 MPa and 22.3± 0.2 % strain). On the other hand, Figure 10(b) shows that the welds prepared using Ti-15-3-0.5C exhibit higher strength (YS = 746 ± 3 MPa, UTS = 755 ± 3 MPa) and ductility (20.7 ± 0.5 % strain) compared to the welds prepared using Ti-15-3-0.25B (YS = 767 ± 5 MPa, UTS = 791 ± 5 MPa and 5.0 ± 0.6 % strain). The autogenous welds show considerably reduced strength (YS = 676 ± 5 MPa, UTS = 734 ± 3 MPa) and ductility (16.4 ± 0.5 % strain) compared to all the other welds because of their coarse grain weld microstructure. The higher tensile strength displayed by the welds with B added and C added fillers compared to autogenous welds could be due to the presence of insoluble particles viz., TiC and TiB, along grain boundaries and within grain and grain refinement in the FZ.

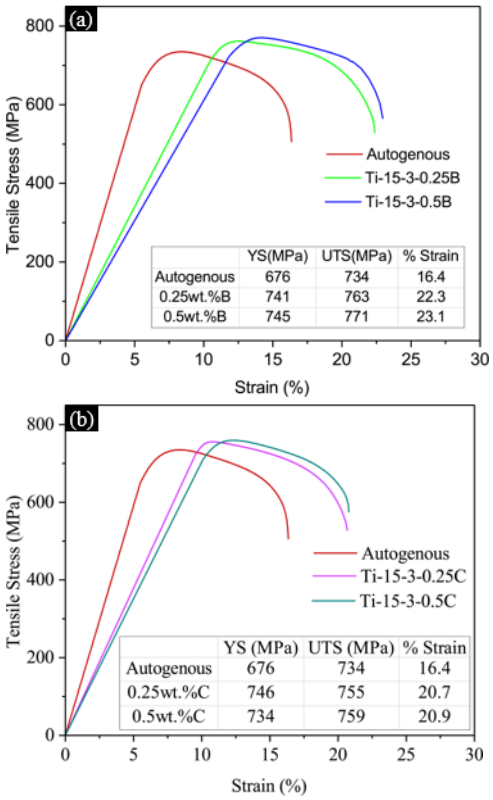

Fig. 10: Tensile curves of Ti-15-3 welds: (a) B added fillers (b) C added fillers

4. Conclusions

Using GTAW method, Ti-15-3 alloys plates have been successfully welded autogenously and using Ti-15-3-xB and Ti-15-3-xC (x= 0.25 and 0.5 wt.%) fillers. XRD, OM, FESEM analysis, hardness and tensile investigation was carried out in the samples. The summaries of results are as follows.

Growth restriction factor of B and C has been suggested to be the mechanism for the grain refinement for hypoeutectic compositions. The addition of B and C in Ti-15-3 caused the formation of TiB and TiC along the grain and inside the grain due to eutectic mixture trapped at intergrain and interdendrite regions.

XRD analysis showed the presence of TiB and β-Ti phases in welds prepared using B added Ti-15-3 alloy fillers while welds prepared using C added Ti-15-3 alloy fillers showed the presence of TiC and β-Ti phases in the FZ.

Introduction of B and C in the weld resulted in higher hardness due to grain refinement and the formation of TiB and TiC precipitates in the FZ. The hardness increased as the amount of B and C addition increased.

Tensile properties improved with addition of B and C in the FZ of weld.

Acknowledgement

Authors would like to thank the financial and facilities support provided by Universiti Teknologi MARA, Malaysia.

References

[1] G. Lutjering & J.C. Williams, “Titanium,” 2007.
[2] C. Leyens and M. Peters, *Titanium an Titanium Alloys*. 2003.
[3] R. R. Boyer, “An overview on the use of titanium in the aerospace industry,” *Mater. Sci. Eng. A*, vol. 213, no. 1–2, pp. 103–114, 1996.
[4] R. Sarkar, P. Ghosal, K. Muraleedharan, T. K. Nandy, and K. K. Ray, “Effect of boron and carbon addition on microstructure and mechanical properties of Ti-15-3 alloy,” *Mater. Sci. Eng. A*, vol. 528, no. 13–14, pp. 4819–4829, 2011.
[5] M. A. Greenfield and D. S. Duvall, “Welding of an Advanced High Strength Titanium Alloy,” *Weld. Res. Suppl.*, no. March, pp. 73–80, 1975.
[6] K. Balachandar, V. S. Sarma, B. Pant, and G. Phanikumar, “Microstructure and mechanical properties of gas-tungsten-arc-welded Ti-15-3 beta titanium alloy,” *Metall. Mater. Trans. A Phys. Metall. Mater. Sci.*, vol. 40, no. 11, pp. 2685–2693, 2009.
[7] V. Balasubramanian, V. Jayabalan, and M. Balasubramanian, “Effect of current pulsing on tensile properties of titanium alloy,” *Mater. Des.*, vol. 29, no. 7, pp. 1459–1466, 2008.
[8] M. Balasubramanian, V. Jayabalan, and V. Balasubramanian, “Developing mathematical models to predict tensile properties of pulsed current gas tungsten arc welded Ti-6Al-4V alloy,” *Mater. Des.*, vol. 29, no. 1, pp. 92–97, 2008.
[9] W. A. Baeslack III and C. M. Banas, “A Comparative Evaluation of Laser and Gas Tungsten Arc Weldments in High-Temperature Titanium Alloys,” *Weld. Res. Suppl.*, no. July, pp. 121–130, 1981.
[10] N. Kishore Babu, S. Ganesh Sundara Raman, R. Mythili, and S. Saroja, “Correlation of microstructure with mechanical properties of TIG weldments of Ti-6Al-4V made with and without current pulsing,” *Mater. Charact.*, vol. 58, no. 7, pp. 581–587, 2007.
[11] M. J. Bermingham, S. D. McDonald, K. Nogita, D. H. St. John, and M. S. Dargusch, “Effects of boron on microstructure in cast titanium alloys,” *Scr. Mater.*, vol. 59, no. 5, pp. 538–541, 2008.
[12] Srinivasan Raghavan and T. Sesh, “Influence of trace boron addition on the directional solidification characteristic of Ti-6Al-4V,” *Scr. Mater.*, vol. 63, no. 12, pp. 1244–1247, 2010.
[13] T. M. T. Godfrey, a Wisbey, P. S. Goodwin, and K. Bagnall, “Microstructure and tensile properties of mechanically alloyed Ti – 6A1 – 4V with boron additions,” *Mater. Sci. Eng. A*, vol. 282, no. 2000, pp. 240–250, 2000.
[14] W. Chen and C. J. Boehlert, “The elevated-temperature fatigue behavior of boron-modified Ti-6Al-4V(wt.%) castings,” *Mater. Sci. Eng. A*, vol. 494, no. 1–2, pp. 132–138, 2008.
[15] S. Tamirisakandala, R. B. Bhat, J. S. Tiley, and D. B. Miracle, “Processing, microstructure, and properties of beta titanium alloys modified with boron,” *J. Mater. Eng. Perform.*, vol. 14, no. 6, pp. 741–746, 2005.
[16] I. Sen, S. Tamirisakandala, D. B. Miracle, and U. Ramamurty, “Microstructural effects on the mechanical behavior of B-modified Ti-6Al-4V alloys,” *Acta Mater.*, vol. 55, no. 15, pp. 4983–4993, 2007.
[17] Z. X. Du, S. L. Xiao, P. X. Wang, L. J. Xu, Y. Y. Chen, and H. K. S. Rahoma, “Effects of trace TiB and TiC on microstructure and tensile properties of ?? titanium alloy,” *Mater. Sci. Eng. A*, vol. 596, pp. 71–79, 2014.
[18] B. Cherukuri, R. Srinivasan, S. Tamirisakandala, and D. B. Miracle, “The influence of trace boron addition on grain growth kinetics of the beta phase in the beta titanium alloy Ti-15Mo-2.6Nb-3Al-0.2Si,” *Scr. Mater.*, vol. 60, no. 7, pp. 496–499, 2009.
[19] R. Banoth, R. Sarkar, A. Bhattacharjee, T. K. Nandy, and G. V. S. Nageswara Rao, “Effect of boron and carbon addition on microstructure and mechanical properties of metastable beta titanium alloys,” *Mater. Des.*, vol. 67, pp. 50–63, 2015.
[20] C. Huang and S. Kou, “Partially Melted Zone in Aluminum Welds — Liquation Mechanism and Directional Solidification,” *Weld. Res.*, no. May, pp. 113–120, 2000.
[21] J. N. Dupont, “Dilution in Fusion Welding,” *ASM Handbook, Weld.*

Fundam. Process., vol. 6A, pp. 115–121, 2011.
[22] S. Tamirisakandala, R. B. Bhat, J. S. Tiley, and D. B. Miracle, "Grain refinement of cast titanium alloys via trace boron addition," *Scr. Mater.*, vol. 53, no. 12, pp. 1421–1426, 2005.
[23] H. J. Z. Albersten, K, Schaller, "No Title," *Z Met. 86*, 1995.
[24] M. J. Bermingham, S. D. McDonald, D. H. StJohn, and M. S. Dargusch, "Beryllium as a grain refiner in titanium alloys," *J. Alloys Compd.*, vol. 481, no. 1–2, pp. 20–23, 2009.
[25] V. Raghavan, *Materials Science and Engineering, A First Course*. 2010.
[26] T. Gladman, "Precipitation hardening in metals," *Mater. Sci. Technol.*, vol. 15, no. 1, pp. 30–36, 1999.